IEEE Access
Multidisciplinary | Rapid Review | Open Access Journal

Received 3 November 2024, accepted 12 December 2024, date of publication 18 December 2024,
date of current version 30 December 2024.

Digital Object Identifier 10.1109/ACCESS.2024.3519513

RESEARCH ARTICLE

All-Encompassing Bone Recognition and Safety Control Strategy for Robot-Assist Laminectomy Based on Milling Force

CHENGAO GAO[1], YU GAO[2], JIAHAO LI[1], YULONG QIN[2], YUFAN ZHAO[3], BAODUO GENG[4], JUNCHEN WANG[1], YONGLIANG YANG[2], DA-WEI DING[2], (Senior Member, IEEE), JILIANG ZHAI[1], AND YU ZHAO[1,5]

[1]Department of Orthopaedic Surgery, Peking Union Medical College Hospital, Chinese Academy of Medical Sciences and Peking Union Medical College, Beijing 100032, China
[2]School of Automation and Electrical Engineering, University of Science and Technology Beijing, Beijing 100083, China
[3]Key Laboratory of Information System and Technology, Beijing Institute of Control and Electronic Technology, Beijing 100038, China
[4]School of Mechanical Engineering and Automation, Beihang University, Beijing 100191, China
[5]State Key Laboratory of Common Mechanism Research for Major Diseases, Beijing 100005, China

Corresponding authors: Jiliang Zhai (zhaidoctor@126.com), Da-Wei Ding (ddaweiauto@163.com), and Yu Zhao (zhaoyupumch@163.com)

This work was supported in part by the National Key Research and Development Program of China, China, under Grant 2022YFB4700700; and in part by the National High Level Hospital Clinical Research Funding under Grant 2022-PUMCH-C-035.

This work involved human subjects or animals in its research. Approval of all ethical and experimental procedures and protocols was granted by the Peking Union Medical College Hospital under Application No. XHDW-2020-024.

ABSTRACT The incidence of spinal degenerative diseases is increasing yearly, due to the global population aging. Spinal surgery, such as laminectomy, remains the most effective, comprehensive, and widely practiced treatment for spinal degenerative disease. As the lamina is adjacent to the spinal cord, spinal nerve injury is one of the most common complications of freehand laminectomy. In view of the high risk, complexity, and extensive learning curve of laminectomy, the surgical robots can improve the safety of surgical operation and have been gradually applied in orthopedics. However, robotic automated laminectomy was challenging because accurate state recognition and safety control are the prerequisites for robotic control, which lack of mature research. Accurate recognition of the inner cortical bone and precise robotic control are key to ensure that lamina is not pierced, which can prevent spinal nerve injury. Therefore, we took the lead in proposing a bone recognition model based on extreme learning machine (ELM) to recognize bone substance for various lamina milling conditions effectively. Specifically, the proposed model captures the features of milling force in spatial order data to produce richer bone characteristics representations. Also, based on our model, a control strategy was proposed to ensure robots stop timely when the milling instruments contact with the inner cortical bone. We verified the effectiveness of our recognition model and control strategy by in vivo and in vitro experiments and obtained great bone recognition performance. Notably, the recognition accuracy reached 100% under most milling conditions. And the laminectomy conducted by robot-assist automatic was controlled more safely than freehand (P value 2.2110−5 and 1.7510−5).

INDEX TERMS Laminectomy, extreme learning machine, universal bone recognition, robot-assist surgery, safety control.

I. INTRODUCTION

Spinal stenosis refers to spinal canal stenosis and subsequent nerve compression, affects nerve functionality [1]. It may also compress the spinal cord's supplying blood vessels leading to hypoperfusion [2], [3]. Lumbar spinal stenosis (LSS) is prevalent and often leads to neurogenic claudication [4]. Cervical spinal stenosis often leads to spinal cord compression and cervical spondylotic myelopathy [5]. Thoracic spinal stenosis is relatively rare, but the prognosis is poor, with

The associate editor coordinating the review of this manuscript and approving it for publication was Yangmin Li.

limited blood supply to the thoracic vertebrae [6]. When treating severe spinal stenosis, laminectomy is the most common and effective treatment for severe spinal stenosis, with a cost-benefit ratio superior to other treatment strategies [7], [8], [9]. Laminectomy is a surgical procedure in which a portion of the lamina is removed to dilate the spinal canal, alter the contours of the spine or allow access to deeper tissue [10], [11], [12]. However, as the lamina is adjacent to the spinal cord, laminectomy bear the risk of intraoperative dural injuries [13], [14], or mechanical injury to the spinal cord or blood vessels [14]. Therefore, preventing intraoperative lamina wear has become a key research focus. With the development of surgical robots, many researchers have begun to study robot-assisted laminectomy, which mainly focuses on milling strategy and control technique for safety reasons [15]. Using force control, researchers realized that the robot stopped operating when the lamina remained 0.9 to 2.2 mm [16], [17]. Deng et al. recognized the bone layers of the lamina with a recognition rate of 86.7-100 % by force sensing [18]. Dai et al. controlled the residual lamina between 0.76-1.51mm through vibration sensing [19]. Dai et al. also achieved a recognition rate of 85.0-95.0% through voice recognition [20]. However, these recognition methods are only suitable for a single grinding tool or even a single milling state, limiting the algorithm's universality.

At present, the bone recognition algorithm based on neural networks mainly uses feedforward neural networks. However, most of the feedforward neural networks are deterministic algorithms and are prone to getting stuck in local optima, especially in deep neural networks with many parameters. This results in lower training efficiency, making them less suitable for real-time and high-precision tasks such as bone recognition surgery. In contrast, the Extreme Learning Machine (ELM) is a single-hidden-layer neural network. The parameters of its hidden layer (weights and biases) are randomly initialized and do not require iterative training adjustments. This gives ELM a significant advantage in training efficiency since it can rapidly perform forward propagation. Additionally, the single-hidden-layer structure of ELM is typically less susceptible to overfitting, as its parameter initialization is random.

ELM is a new training algorithm in feedforward neural networks [21], which is widely used in biomedicine. For example, ELM using Differential Evolution Algorithm (DEA-ELM) [22] was executed to improve the classification accuracy of electrocardiogram signals. ELM using in the major histocompatibility complex (ELM-MHC) [23] achieved higher accuracy in the recognition of major histocompatibility complexes by combining ELM and bioinformatics analysis technology. ELM classifier was used [24] to improve the speed and reliability of predicting RNA-protein interactions. Han et al. [25] extracted the gene-to-class sensitivity information from the samples by ELM to improve the interpretability of the selected genes in traditional gene selection methods and prediction accuracy. The method [26] used an ELM-based weighted probabilistic model to improve the performance of the classification of the electroencephalography (EEG) signals in synchronous brain–computer interface (BCI) system. Compared with the traditional feedforward neural network algorithm based on gradient descent, ELM has the advantages of strong generalization, fast learning speed, and avoiding falling into local minimum points, which has become a research hotspot in artificial intelligence. The essence of the bone recognition task is to predict the type of bone to be ground. There are many milling conditions in laminectomy. Therefore, the designed algorithm should not only achieve online accurate prediction, but also ensure universality.

Inspired by the above observations, this article presents a novel all-encompassing bone recognition model extracting milling force features learning for safety control strategy for robot- assisted laminectomy. The presented model follows an end-to-end structure. Specifically, to capture the sophisticated bone characteristics, we design a fitting module to extract the features of milling force in spatial order, effectively reflecting the density difference of different bones. The proposed fitting module preliminarily predicts the bone substances to be milled at the next moment. Also, we propose a classification module, which adeptly amalgamates force features across various milling conditions and avoids interference with the universality of the model caused by different surgical tools. Through the classification module, bone characteristic is further captured. Therefore, the all-encompassing recognition ability of the network is more prominent. In addition, a data enhancement algorithm is applied to improve recognition accuracy by expanding the amount of the sample of inner cortical bone and its underside. This data enhancement algorithm solves the problem of data positive and negative sample ratio imbalance in the training processing. Finally, in order to verify the performance of our bone recognition algorithm and safety control strategy in real surgical scenarios, animal experiments on swine were carried out for each milling condition. The results demonstrate the superior ability of our bone recognition method to discern cortical bone in the inner lamina and the precision of the safety control strategy to control robotic milling. Our contribution is summarized as follows.

1) We proposed a bone recognition model based on ELM. This model excelled in the efficient and accurate recognition of bone composition under diverse milling conditions. The method integrated fitting and classification modules to extract milling force features from the spatial order, thereby creating a richer representation of skeletal characteristics.
2) We implemented a data augmentation strategy for enhanced performance. By expanding the dataset for inner cortical bone and its underlying types, the issue of imbalance between positive and negative samples in the dataset was addressed, which led to an improvement in recognition performance.

3) The aforementioned bone recognition model and data augmentation method were validated through in vitro and in vivo animal experiments. The results demonstrated that we established a safe control strategy, compiled a force dataset, and confirmed its superior performance in bone recognition. The precision and versatility of the recognition algorithm were validated, as were the stability and safety of the control strategy. This framework was well-suited for controlling autonomous robots to assist in laminectomy.
4) The rest of this article is organized as follows. Section II reviews related work, and the section III explains the construction and training process of our algorithm in detail. In section IV we describe the results of evaluation and validation using simulation experiments and animal experiments. The conclusion is presented section V.

II. RELATED WORK

We briefly review the recent progress and applications of neural network-based bone recognition methods and force-based grinding control strategies.

A. BONE RECOGNITION METHOD BASED ON NEURAL NETWORK

Bone recognition stands as a pivotal and indispensable task in spinal surgery, especially in laminectomy, where it is an essential reference factor for stopping bone milling or drilling and is related to the safety of surgery [27]. Specifically, a Back-Propagation (BP) neural network was applied to recognize cancellous bone and cortical bone according to audio signals during bone drilling, realizing bone layer recognition during pedicle screw implantation [28]. Due to the mathematical relationship between milling force and depth [29], a BP neural network based on multi-information training, including milling force and number of layers, was applied to bone recognition in laminectomy. The influence of multiple characteristics on bone recognition was comprehensively considered to improve the safety and reliability of robotic-assisted laminectomy [30]. Long short term memory (LSTM)can recognize and judge grinding conditions based on sound and grinding force signals [31]. In addition, some researchers used the Radial Basis Function (RBF) algorithm to realize bone recognition in the drilling process based on sound and grinding force signals [32]. However, most of these algorithms adopt the gradient descent method, which will lead to the problems of slow training speed, needing help to reach the global minimum, and selection sensitivity of the learning rate. Moreover, these algorithms have yet to solve the problem of many kinds of working conditions of generality, mostly due to a lack of animal experiments.

B. FORCE-BASED MILLING CONTROL STRATEGY

The control strategy is another fundamental step to realize the robot-assisted laminectomy, because it is the basis of robot-autonomous bone milling. Specifically, according to the difference in milling force between cortical and cancellous bone, researchers constructed a robot force control system to control the robot to maintain a prudent safety margin [16]. In light of the complexity of spinal surgery, some studies have proposed a fuzzy control strategy based on milling force to adjust the feeding speed and feeding depth online to protect the lamina from penetration [17]. In addition, multistage fuzzy control (MLFC) has also been applied to bone milling to achieve more stable and efficient milling than freehand and stop the inner cortical bone accurately [33]. However, a neural network-based control strategy has stronger adaptability and robustness. Moreover, these control strategies have yet to be verified on live animals, and in the case of live animals, surgery than fixed bone in vitro experiments are more complicated.

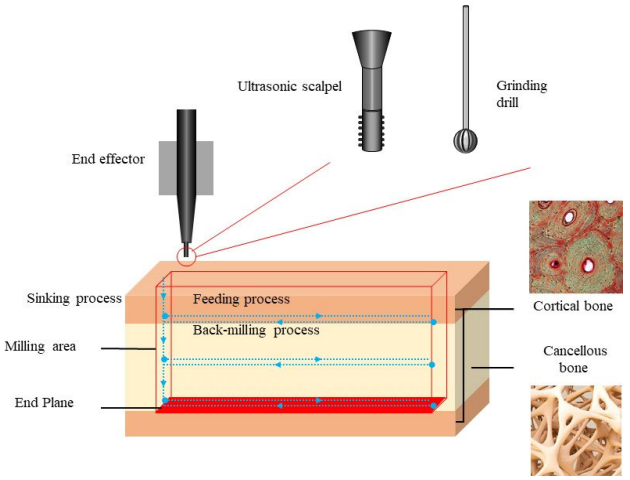

FIGURE 1. Bone structure ideogram of the vertebral plate and milling strategy. The lamina includes two cortical bone layers and one cancellous bone layer. The orange part is cortical bone, and the yellow part is cancellous bone. The milling strategy is that the robot end-effector carries a grinding drill or ultrasonic scalpel to grind the vertebral plate layer by layer. The blue dotted line is the milling path, the red solid line is the milling area, and the red parallelogram is the plane where the milling stops.

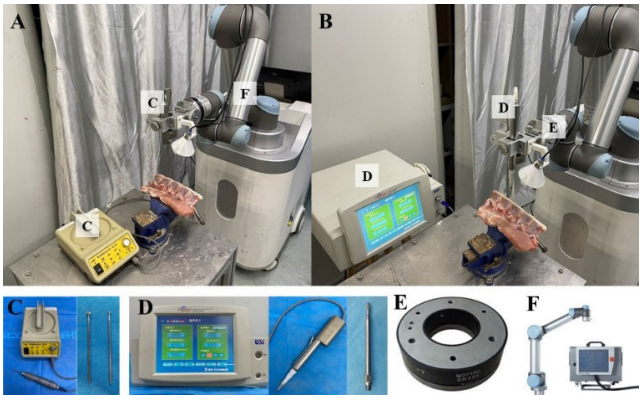

FIGURE 2. Milling platform. The platform consists of robotic arms, force sensors, computers, control systems and milling tools. A. Milling platform loaded with grinding drill. B. Milling platform loaded with ultrasonic scalpel. C. Grinding drill and the controller. D. Ultrasonic scalpel and the controller. E. Force sensor. F. Robot arm.

III. THE STATE RECOGNITION ALGORITHM

A. BONE LAYER ANALYSIS AND FORCE SIGNAL ACQUISITION

The bone structure of the lamina is mainly composed of cortical bone and cancellous bone, as shown in Fig. 1. In the process of laminectomy, the robot controlled the surgical equipment to mill the lamina along the outer cortical bone and cancellous bone, which is operated layer by layer. In order to alleviate the weakening of the mechanical properties of the spine, the operation was ultimately terminated in the inner cortical bone. Therefore, it is particularly important to accurately recognize the intraoperative status and ensure that the milling operation can be terminated in time during the operation.

In general, cortical bone has good mechanical properties and plays an important role in supporting the body and protecting organs. Cancellous bone, meanwhile, is a soft tissue with low density and elasticity that evenly fills the inner areas of the cortex, helping to maintain bone shape and resist external stress. Van Ham et al. [34] found that the two bone structures exhibit different mechanical properties during surgery, which provides us with the possibility to recognize the surgical state. The purpose of this study is to extract the characteristics of force signals collected during surgery and realize the recognition of intraoperative states after subsequent processing.

The system that collects force signals mainly consists of two parts: a platform of lamina milling and a force signal detector sensor. The platform of lamina milling is a six-degree-of-freedom robotic arm that combines a position servo control system and a milling scalpel (Fig. 2). In this study, we choose the collaborative Danish Universal Robots 5 (UR5), which provides a stable and reliable operation for lamina milling with high performance on repeated accuracy, braking and moment of inertia. We choose an M8128 force sensor (US SRI) as the force signal detector sensor to collect the force signal at the end of the manipulator in real-time. The M8128 force sensor uses a six-axis force sensor to simultaneously measure three forces and three moments in the inertial coordinate system and collect milling force signals from various angles. The force sensor consists of an inner ring, outer ring, force measuring beam, and strain gauge. When there is a relative force between the inner and outer rings, the strain gauge detects the generated external force using the force measuring beam, converts it into an electrical signal, and outputs it to the acquisition card. The force measurement accuracy was within 2% FS. The digital acquisition card used a 24-bit sigma-delta analog-to-digital converter with a sampling frequency of up to 2 kHz to discretize the analog output of the force sensor, which was then sent to the host computer for processing through the RS232 protocol.

B. PREPARATION OF FORCE DATA

1) FORCE SIGNAL ACQUISITION

The force signals during the milling process are generated by friction between the scalpel and the bone layer. In order to extract a characteristic amount of the force signal and perform subsequent processing, the generated signal needs to be collected. During the experiment, the above experimental device is used to collect the signal. The sampling frequency is set to 100HZ. The relationship between the spatial coordinate axes of force and the trajectory of the scalpel's movement is shown in Fig.3. When the scalpel is not in contact with the bone layer, the force signal is minimal. The moment the scalpel makes initial contact with the bone, the force signal increases sharply. After the scalpel penetrates the outer cortical bone, the force signal noticeably decreases. This phenomenon is attributed to the higher bone density and hardness of the cortical bone, resulting in a higher force signal compared to the intermediate cancellous bone. When the scalpel makes contact with the inner cortical bone, the force signal once again increases significantly. On this basis, we can select the force signal during the period from the beginning of contacting the outer cortical bone to drilling through the inner cortical bone, and process the selected signal in the time domain. The selected signal in the time domain during the process is shown in Fig. 4.

It can be seen from the figure that the data distribution of force signals is relatively dense, and there is obvious noise in the original force signals. It is difficult to distinguish the differences between bone layers using the original force signals. Therefore, it is necessary to process the original signals to obtain the characteristics of the force signals during the operation to recognize different bone layers.

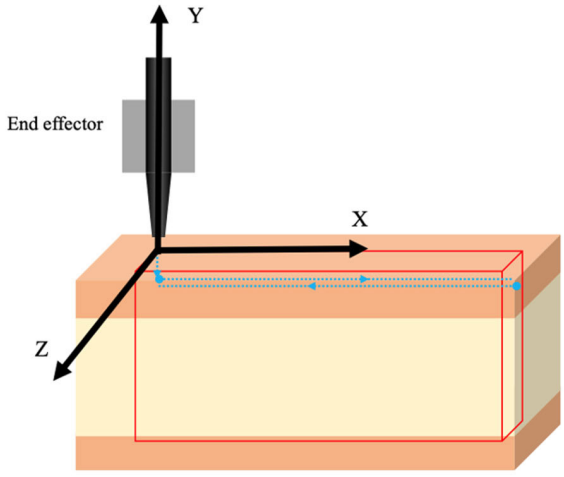

FIGURE 3. The relationship between the spatial coordinate axes of force and the trajectory of the scalpel's movement.

2) PRE-PROCESSING OF THE FORCE SIGNAL

Force sensors measure the interaction force between the surgical equipment and the vertebral lamina with a sampling frequency of 100HZ. Due to the influence of motor vibration and other factors, the original force signal contains many types of noise, which will cause a very adverse effect on the experiment, so the collected force signal needed to be

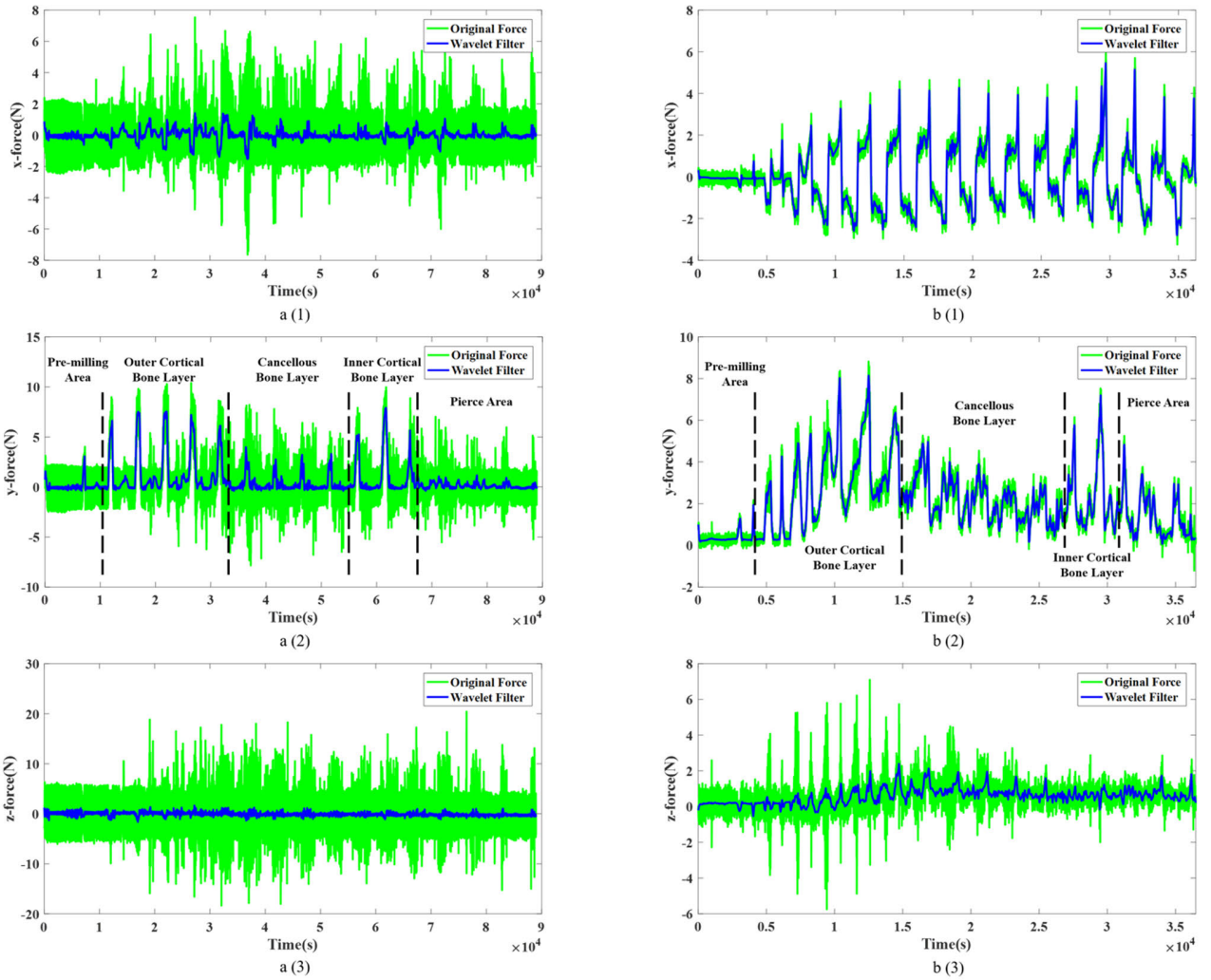

FIGURE 4. Comparison of force signals before and after filtering. Figure a shows the force signal based on the grinding drill. Figure b shows the force signal based on the ultrasonic scalpel. The force values in the x-direction are shown in a (1) and b (1), the force in the y-direction is shown in a (2) and b (2), and the force in the z-direction is shown in a (3) and b (3).

pre-processed before subsequent processing. In this article, we process the original force signal by wavelet filtering to suppress the periodic interference and get the filtering result with high smoothness. The signal is decomposed by a three-layer wavelet based on a Daubechies DB3 wavelet basis. The data after wavelet decomposition are processed by the rigrsure threshold denoising function and soft threshold rule, and then the decomposed data are reconstructed to obtain the filtered signal. The comparison effect before and after filtering is shown in Fig. 4.

3) ANALYSIS AND FEATURE SELECTION OF THE FORCE SIGNAL

The purpose of this article is to recognize the intraoperative accurately state to determine whether the current milling procedure has proceeded to the inner cortical bone. We regard the completion of the one-layer milling procedure as a basic operation unit of lamina milling, which consists of three operations: downward, forward, and backward. In order to more accurately recognize the bone substance under various milling conditions, in this study, we select the resultant force in X and Y directions of the forward process as the force characteristic input of the model. In addition, at the beginning and end of each milling layer, there would be force signal fluctuations caused by external interference of the system, so we apply corrections to the initial and final 20% of the data in each layer, filtering out data exceeding the threshold. In order to give full play to the powerful fitting ability of the model, we introduce temporal features of force signals to improve the performance of the model. In this article, we have chosen ''numbers of milling layer'' as a temporal feature. Each layer represents the time required to complete one full cycle of downward, forward, and backward operating units. The number of milling layers is generated by counting basic operation unit. It contains rich temporal information and contextual features of force data.

C. THE BONE RECOGNITION ALGORITHM

1) ALGORITHM BASED ON ELM

Compared with the traditional feedforward neural network algorithm based on gradient de- scent, ELM has the advantages of strong generalization, fast learning speed, and avoiding falling into local minimum points. Moreover, the weights in the ELM algorithm can be generated randomly, which reduces the cost of adjusting parameters. ELM has become a research hotspot in the field of artificial intelligence. The function of our algorithm is to predict whether the inner cortical bone will be milled at the next moment of the lamina milling process. Our algorithm is applicable to both ultrasonic scalpels and grinding drills. We take the characteristic force signal and layers as the input of the algorithm to extract the characteristics of force values in spatial order. The model will output the current bone substance based on the force characteristics at the moment. Specifically, ELM algorithm is used to predict bone substance according to force value and milling layer number. The output of algorithm is floating point value at this time, then, these values are dichotomized by ELM, and the classification results are used as the final model output.

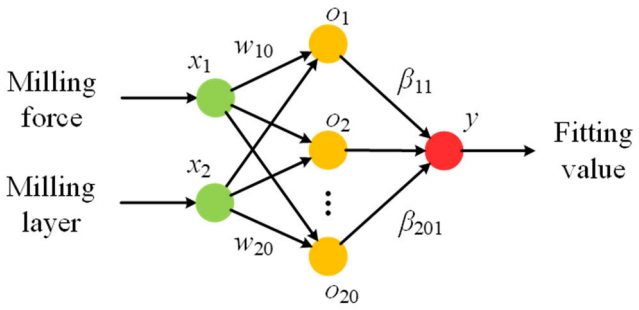

FIGURE 5. ELM structure of fitting process. The fitting process is a single-hidden-layer structure, consisting of 20 neurons. The input consists of milling force and the milling layer count, while the output is the fitted value.

The modeling steps are as follows.

2) STEP1: FITTING PROCESS

The network structure of the fitting process is shown in the Fig. 5, x_1 and x_2 are the input elements of the neural network, corresponding to the characteristic milling force, the layer number of milling, respectively, and y is the output. To judge whether the current milling layer is the innercortical bone, the output value is set to 0 or 1. w_{1o}-w_{20o} are the weights from the input layer to the hidden layer, and β_{11}-β_{201} are the weights from the hidden layer to the output layer.

Suppose there are Q different training samples $(x_q,\ t_q)$, where $x_q = [x_q1,\ x_q2,\ldots,\ x_{qn}]^T \in \mathbf{R}^n$ is the input matrix, $t_q = [t_q1,\ t_q2,\ldots,\ t_{qm}]^T \in \mathbf{R}^m$ is the corresponding expected output matrix. We use n to represent the number of input neurons, m to represent the number of output neurons, and l to represent the number of hidden layer neurons. Hidden layer activation function $g(x)$. ELM mathematical model can be expressed as:

$$H\beta = T \tag{1}$$

where, H is the hidden layer output matrix, which can be expressed as:

$$H = \begin{bmatrix} g(\omega_1 \cdot x_1 + b_1) & \cdots & g(\omega_1 \cdot x_1 + b_1) \\ \vdots & \ddots & \vdots \\ g(\omega_1 \cdot x_1 + b_1) & \cdots & g(\omega_1 \cdot x_1 + b_1) \end{bmatrix}_{Q\times l} \tag{2}$$

where, $\boldsymbol{w}_i = [w_{i1},w_{i2},\ldots,\ w_{il}]^T$ and $\boldsymbol{b}_i = [b_{i1},b_{i2},\ldots,\ b_{il}]^T$ represent the weight matrix and neuron threshold between the i^{th} input layer and the hidden layer, respectively. $\boldsymbol{\beta} = [\beta_{1j},\ \beta_{2j},\ldots,\beta_{lj}]^T$ represents the connection weight matrix between the hidden layer and the j^{th} output layer. $\boldsymbol{T}= [\boldsymbol{t}_1,\ \boldsymbol{t}_2,\ldots,\boldsymbol{t}_Q]^T$ is the expected output matrix for neural networks. When the training set is given and the hidden layer neuron parameters $\boldsymbol{w}_i, \boldsymbol{b}_i$ are randomly generated, the hidden layer output matrix $\boldsymbol{H}$ can be determined and remains unchanged in the subsequent learning process. Therefore, equations (1) can be converted to the least square solution $\hat{\boldsymbol{\beta}}$ of linear system $\boldsymbol{H\beta} = \boldsymbol{T}$

$$\widehat{\beta} = H^{+}T \tag{3}$$

where, $\boldsymbol{H}^+$ is Moore-Penrose generalized inverse of hidden layer output matrix $\boldsymbol{H}$.

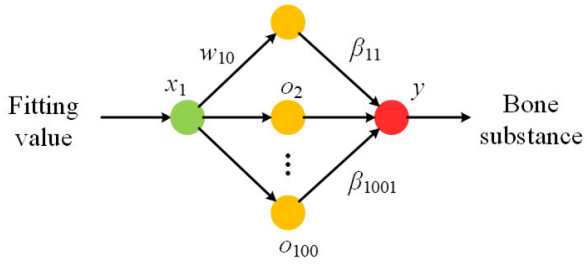

FIGURE 6. ELM structure of classification process. The classification process is also a single-hidden-layer structure, consisting of 100 neurons. The input is the fitted value, and the output is the bone quality category.

TABLE 1. The milling condition of grinding drill.

No.	Grinding drill	
	Milling speed	Rotation speed
1	0.5mm/s	10000r/s
2	0.5mm/s	15000r/s
3	0.5mm/s	20000r/s
4	1mm/s	10000r/s
5	1mm/s	15000r/s
6	1mm/s	20000r/s

The specific steps of ELM bone recognition are as follows:

1) The number of hidden layer neurons is set to 20. The threshold of hidden layer neurons and the connection

TABLE 2. The milling condition of ultrasonic scalpel.

No.	Ultrasonic scalpel	
	Milling speed	Milling power
1	0.5mm/s	60%
2	0.5mm/s	80%
3	0.5mm/s	100%
4	1mm/s	60%
5	1mm/s	80%
6	1mm/s	100%

weight between input layer and hidden layer are randomly set.

2) The activation function of neurons in the hidden layer is determined to be Sigmoidal, so as to calculate the output matrix $\boldsymbol{H}$ of the hidden layer.
3) Calculate the connection weights between hidden layer and output layer.

After getting the weights, the model generates the results of fitting 0 and 1 in the test process, but these results are floating point values. So we need to design a binary classifier to accurately determine the bone substance.

3) STEP2: CLASSIFICATION PROCESS

We build a classification module based on ELM. The principle of the classification task is similar with the test process. In this model, the number of input neurons and output neurons is 1, and the number of hidden layers is set to 100. The module structure is shown in the figure. (Fig. 6). x is the output set of fitting process which combines floating point values, y is set to 0 or 1. In addition, Sigmoidal is still selected as the activation function.

a: TRAINING DETAILS

1) Training data sets
Considering that the biological and mechanical properties of swine spine and vertebra is similar to human's, we chose the swine lamina as the milling object in vitro and in vivo experiments. To establish a dataset for model training, we carried out in vitro swine lamina milling experiments and collect force signals during milling process. In this research, a total of 36 segments of thoracic and lumbar spine, which included 36 laminas, of fresh adult swine purchased from the market were selected. We tested 12 milling conditions with 6 times repeated experiments for each condition. In terms of ultrasonic scalpel, we designed 3 kinds of milling power:100%, 80%, 60% (This percentage represents an adjustable parameter in the device. The ultrasonic scalpel has a maximum power of 150W, where 100% corresponds to a grinding power of 150W, 80% corresponds to 120W, and 60% corresponds to 90W), while for grinding drill, 3 grinding speeds including 10000r/s, 15000r/s, 20000r/s were chosen. Each milling instruments can move in speed of 0.5mm/s and 1mm/s (Table. 1 and 2). Before lamina milling, the muscles and other soft tissues around vertebra were scraped with scalpel, exposing the spinous process, lamina, superior and inferior articular process. The spine was clamped onto a platform to avoid movement (Fig. 2). Starting and ending points, milling path were determined by the surgeon. After milling path confirmed, start the milling system, and collect force signal from six-axis sensor of the whole process simultaneously until the lamina was pierced. The force signal will be recorded, filtered and applied to estimate bone substance.
2) Data augmentation algorithm
In this article, we treat the problem of bone recognition as an abnormality detection problem. When the inner cortical bone is milled, we believe that an abnormality has occurred and the operation must be terminated. Therefore, we consider the training data of the outer cortical and cancellous bones as normal samples and the remaining data as abnormal samples. As shown in Fig. 7, since the number of normal samples is much larger than the number of abnormal samples in a milling data collection process, there is a serious imbalance between positive and negative samples in training data. This will cause that the separation hyperplane is partial to the samples with a large proportion, which will cause over-fitting to the detection with a large number of samples and reduce the generalization ability of the model. Therefore, we need to increase the number of minority samples to get a balanced dataset. Since repeated sampling will add some insignificant negative samples or the repetition of existing negative samples and cause over- fitting, here we use ADASYN [35] to artificially synthesize some new minority samples. Specifically, we first calculate the final number of samples that need to be synthesized, then for each minority sample, its K-nearest neighbor is calculated according to the Euclidean distance, and the weight of the minority sample is determined according to the proportion of the majority sample in the K-nearest neighbor. We calculate the number of new samples that needs to be generated from this sample according to the weight, which can effectively avoid the occurrence of sample aliasing. In particular, in order to avoid the influence of oversampling on the model training process, oversampling need to be used after the division of dataset in cross-validation process.

$$G = \left(S_{maj} - S_{min}\right) \times \beta \tag{4}$$

where S_{maj} stands for the number of major class and S_{min} stands for the number of minority samples, G stands for the number of samples synthesized in this process and β represents the equilibrium coefficient and its value range is $[1, 0]$. If β equals 1, the number

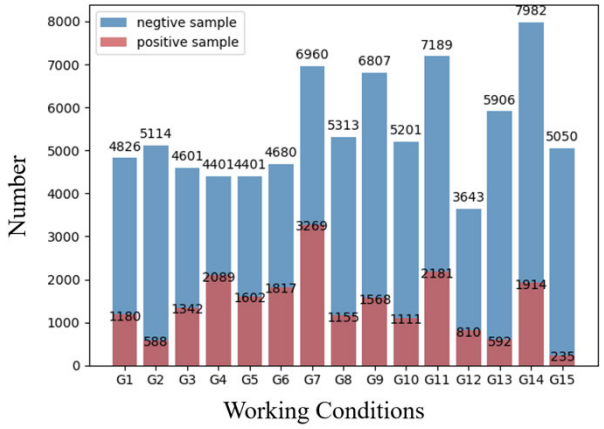

FIGURE 7. Positive sample versus negative sample.

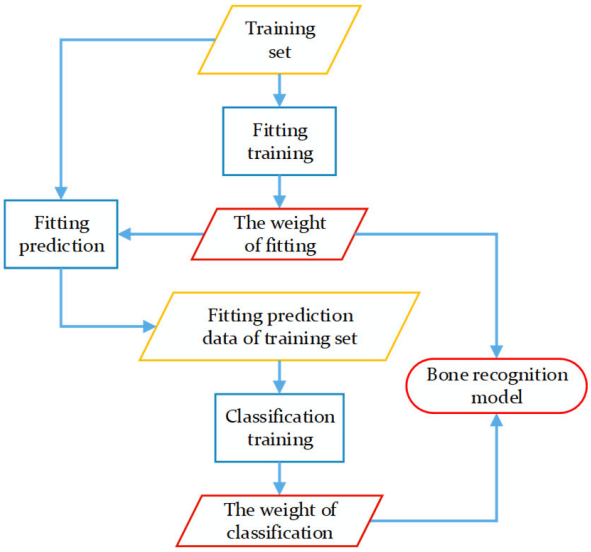

FIGURE 8. Training process of all-encompassing bone recognition model.

of samples is the same after oversampling.

$$\Gamma_i = \frac{\Delta_i / K}{Z} \tag{5}$$

where Δ_i stands for the number of major samples in K nearest neighbors and Z stands for the normalization factor that guarantees that Γ constitutes a distribution. So if a minority sample x_i is surround by a large number of major class, the Γ_i is higher.

$$g_i = \Gamma_i \times G \tag{6}$$

where g_i is the number of samples to be synthesized for each x_i.

3) Model training process
Firstly, the training set is used to train the fitting module, and the fitting weights are recorded. Then, the training set is fitted with the weight values to obtain the prediction results of the training set. Finally, the classification module is trained by the prediction results of the training set, and the classification weights are recorded. Therefore, the training parameters of the model are composed of fitting weights and classification weights. The training process of the bone recognition model is shown in the Fig. 8.

4) Safety Control Strategy
In this study, the ELM was used to establish the laminectomy safety control strategy (Fig. 9.), which controlled the robot to mill the lamina and to stop autonomically. In the process, the force sensor mounted on the end of the robot acquired the force signal in real time. After processing, the force signal, together with the layers recorded in the movement of the robot, was input into the ELM for testing, so as to realize the real-time recognition of the bone substance at the current milling end. The output was 0 when the milling end was located at the non-inner cortical bone, and 1 when reached the inner cortical bone. We configured the ELM to send instructions to the robot every 10 predicted values. When a certain number of these predicted values exceed a threshold and are classified as 1, that is, they are considered to represent the inner cortical bone. the stop instruction will be issued to stop the movement of the robot. This automatic stop strategy can ensure lamina is not be pierced, and the milling instruments do not injure the spinal cord and spinal nerve root, achieve the safety control of the robot assisted laminectomy.

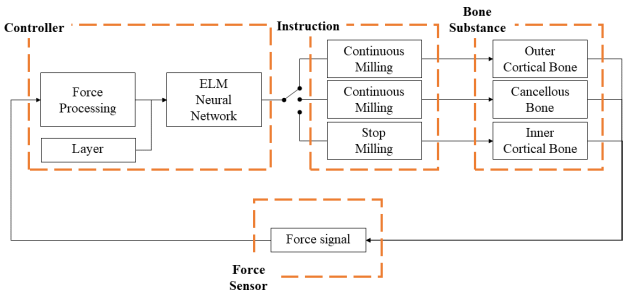

FIGURE 9. Safety control strategy of laminectomy.

IV. EXPERIMENT

To verify the accuracy and feasibility of the model, we carry out simulations and animal experiments. Simulation are experiments based on force characteristic data of the *in vitro* swine lamina. In animal experiments we use real-time force data for model testing. Considering ethical issues, we conduct simulation verification before the live animal experiment. Animal experiments are carried out on the basis of the feasibility of simulation experiments.

A. SIMULATION EXPERIMENT

1) DETAILS OF SIMULATION EXPERIMENT

First, we process the collected force data by executing a wavelet filter to reduce the interference noise. Then we select

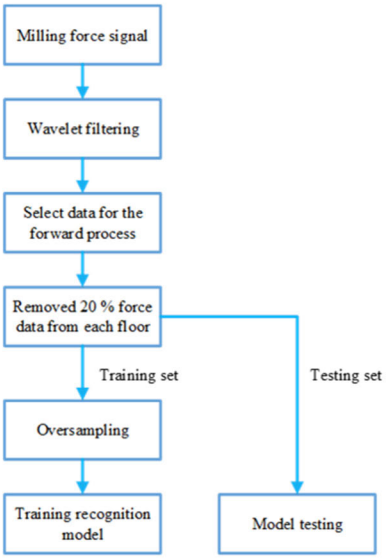

FIGURE 10. Simulation experiment process.

the data from the forward process. Since the force data near the milling starting point contains a large number of interference signals, we remove 20% of the force data at the beginning and end of each layer, and obtain the noise removal data. After oversampling, the amount of data in the inner cortical bone is increased. We build a bone recognition model based on Python language. And the model is trained with over-sampled data and tested with unsampled data.

2) SIMULATION EXPERIMENTAL DATA

All the data used to train the model are collected by the in vitro experiment. In the selected 12 milling conditions, we repeatedly collect 6 groups of data in each milling condition, 1 group of which is used as test set and the rest as training set. This ensures that the training set has enough data. Each condition is included in the test set, so we can verify the universality of the model.

3) EXPERIMENTAL RESULT ANALYSIS

1) Evaluation metrics

Recognition of inner cortical bone can be regarded as an anomaly detection. We regard inner cortical bone and its un- derside as positive and outer cortical bone and cancellous bone as negative. The four metrics in Table 3 can be explained as:

- True positives (TP): Predict inner cortical bone and its underside as inner cortical bone and its underside.
- False positives (FP): Outer cortical bone and cancellous bone is predicted as inner cortical bone and its underside.
- True negatives (TN): Outer cortical bone and cancellous bone is predicted outer cortical bone and cancellous bone. False negatives (FN): Inner cortical bone and its under- side is predicted as outer cortical bone and cancellous bone.

We use two metrics to appraise the performance of bone recognition model: Accuracy and F_1-Score.

- Accuracy: The correct ratio of bone recognition bone for all samples.

$$Accuracy = \frac{TN + TP}{TP + FN + TN + FP} \tag{7}$$

- F_1-Score: Harmonic mean of the precision ratio and the recall ratio. It is used to measure the binary classification capability of the model, and it can be used to quantify the ability of bone recognition model.

$$F_{1\_}Score = 2 \cdot \frac{recall \cdot precision}{recall + precision} \tag{8}$$

$$precision = \frac{TP}{TP + FP} \tag{9}$$

where precision is the ratio of the number of inner cortical bone and its underside samples correctly judged and the total number of inner cortical bone and its underside samples predicted.

$$recall = \frac{TP}{TP + FN} \tag{10}$$

and *recall* is the ratio of the number of inner cortical bone and its underside samples correctly judged by the model to the total number of real cortical bone samples.

TABLE 3. The confusion matrix.

		Predicted Value	
		Positive	**Negative**
Observed Value	**Positive**	TP (True Positive)	FN (False Negative)
	Negative	FP (False Positive)	TN (True Negative)

TABLE 4. Ablation study on different components in our bone recognition model.

	+OS	+CLASS	F1-Score	ACC
Fitting ELM			0.747	84.96
Fitting ELM		✓	0.794	86.76
Fitting ELM	✓		0.791	86.79
Fitting ELM	✓	✓	0.836	89.07

2) Ablation experiments

In model validation, we use sampling points as a unit to do bone recognition. The last line of Table 4 shows the recognition accuracy of the all-encompassing bone recognition model. This data verifies the universality of the model, which means our model can be applied based on both ultrasonic scalpel and grinding drill. It can also be seen from the data in this line that the model has a strong recognition ability for cancellous bone and inner cortical bone. Accurate recognition of

cortical bone is a necessary condition to achieve security control. A high recognition sensitivity for inner cortical bone is reflected by F_1-Score, which ensures that the model can accurately recognize the cortical-cancellous junction.

We investigate the impact of the oversampling algorithm on recognition accuracy, as well as the effectiveness of the classification module in Table 4. We use force data and milling layers to predict bone substance.

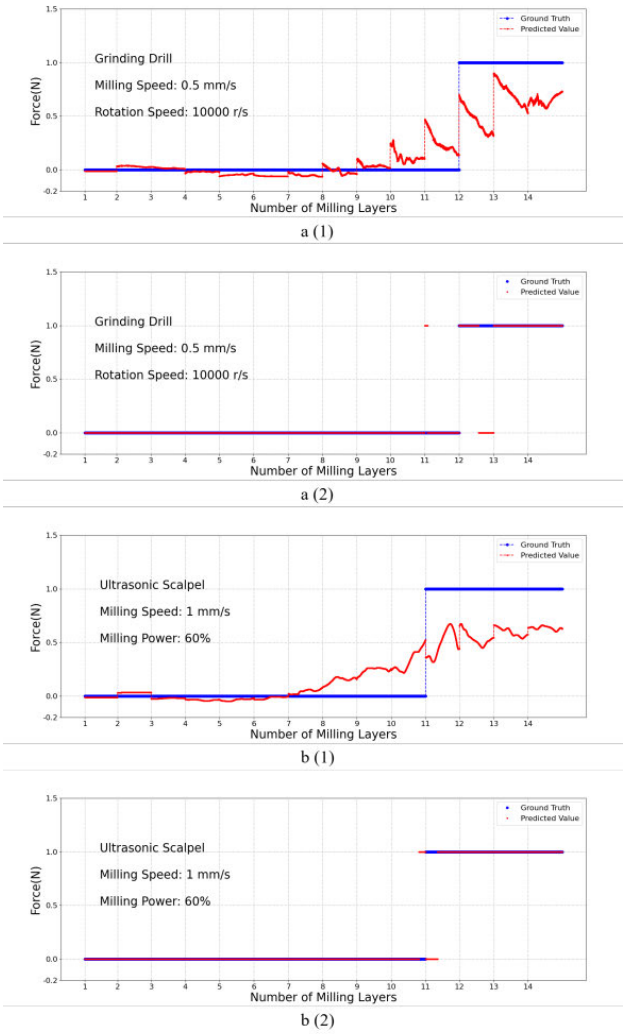

FIGURE 11. The fitting module and the classification module output by sampling points.

We explore 4 possible combinations: without oversampling and classification module, only apply the classification module, only apply the oversampling, and apply both oversampling and classification module. To verify the impact of oversampling, we conduct experiments with and without the classification module. The results in Table 4 demonstrate that our data enhancement algorithm has a significant impact, weakening the problem caused by the imbalance of positive and negative sample ratio. In order to verify the validity of the classification module, experiments are carried out in the case of oversampling being applied and not being applied respectively. For the same fitting output, we use threshold classification (threshold=0.5) and ELM- based classification algorithm to classify the results. ELM-based classification algorithm has stronger overall recognition ability and higher recognition accuracy for inner cortical bone. The artificially set classification threshold is not all-encompassing, and different thresholds should be allocated for different milling conditions. ELM-based classification module has strong adaptive ability, which can avoid the influence of milling conditions and enhance the universality of the algorithm. Comparing the results of these the four combinations in Table 4, it is obvious that the oversampling and classification module improve the performance. The two modules are applied to our model and the best overall effect is achieved.

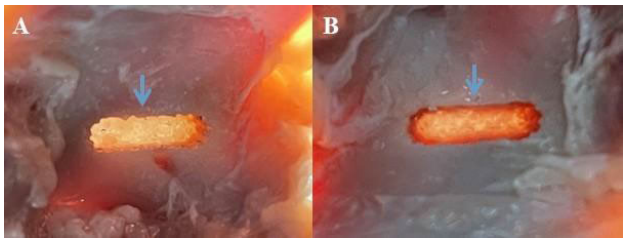

FIGURE 12. Vision observation of in vitro milling results. A. Result of grinding drill. B. Result of ultrasonic scalpel. The blue arrow in the figure are the milling areas.

We record the recognition results in one milling condition of ultrasonic scalpel and grinding drill respectively. Fig. 11 shows the output of the fitting module and the classification module. The first figure of each subgraph shows the result of the fitting process, and the overall trend of the fitting curve is close to true value curve, which reflects the recognition ability of the fitting module. Graph a (2) and b (2) of Fig. 11 show the recognition results of the two milling conditions, and it can be seen that most of the sampling points can be accurately predicted by model, although some sampling points with wrong prediction are generated at the cortical-cancellous junction. In actual operation, we will comprehensively calculate the output signals of multiple sampling points as the stop milling signal of the robot. Therefore, the existing error is within the acceptable range.

B. ANIMAL EXPERIMENT VERIFICATION

1) IN VITRO VERIFY EXPERIMENT

To verify the security and accuracy of our stop control strategy, we have carried out the *in vitro* experiment and *in vivo* experiments on live animals successively. The subjects and conditions of the in vitro experiment were almost the same

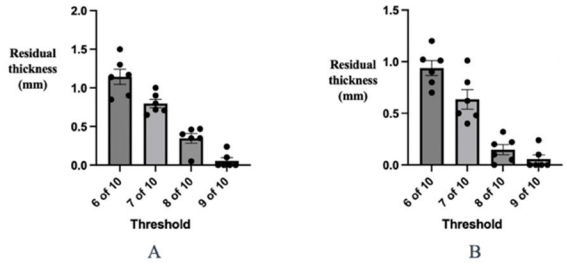

FIGURE 13. Residual thickness of lamina under different thresholds. A. using ultrasonic scalpel. B. using grinding drill.

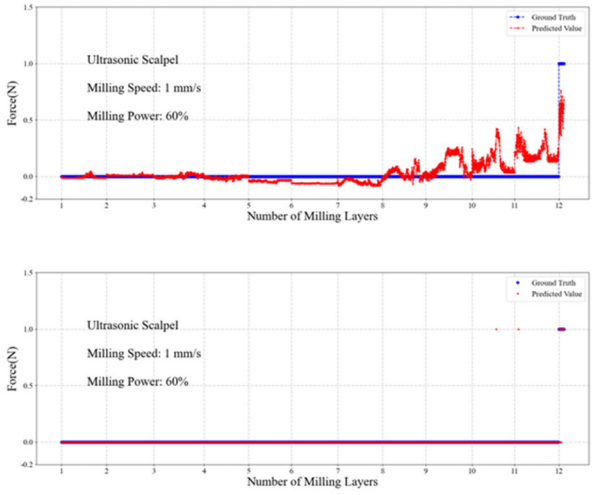

FIGURE 14. The fitting module and classification module output by sampling points in the in vitro experiment. (Threshold: 8 of 10).

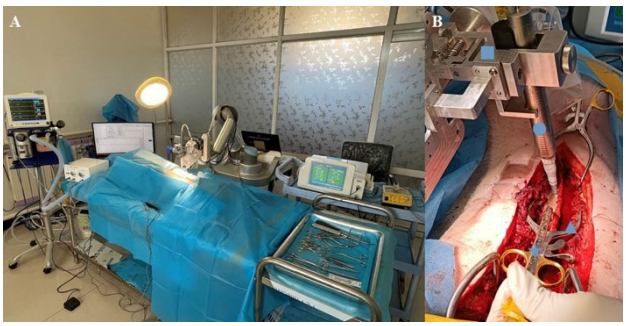

FIGURE 15. IN VIVO experiment. A. The in vivo experimental environment including anesthesia machine, ventilator operating-lamp, surgical instrument, surgical robot. B. Milling procedure of robot-assist laminectomy.
■. End of robot arm. •. Milling tool. ⋆. Aspirator ▲. Spreader.

as the process of building training sets. The only difference is that in verified experiment, milling process ends when the algorithm determines that the grinding instruments reaches the inner cortical bone of lamina according to the force signal collected in real time, rather than the lamina is pierce. This strategy theoretically results in only the inner cortical bone is left, which not only facilitates subsequently lamina detachment but also ensures the safety of laminectomy. We set

TABLE 5. *IN VITRO* result of grinding drill.

No.	Residual thickness (mm)	Pierce rate	Thick rate (>1.0mm)
1	0.43±0.07	0.00% (0/3)	0.00% (0/3)
2	0.30±0.10	0.00% (0/3)	0.00% (0/3)
3	0.31±.0.09	0.00% (0/3)	0.00% (0/3)
4	0.45±0.08	0.00% (0/3)	0.00% (0/3)
5	0.31±0.17	0.00% (0/3)	0.00% (0/3)
6	0.38±.0.08	33.33% (1/3)	0.00% (0/3)
Total	0.36±.0.11	5.56% (1/18)	0.00% (0/18)

TABLE 6. *IN VITRO* result of ultrasonic scalpel.

No.	Residual thickness (mm)	Pierce rate	Thick rate (>1.0mm)
1	0.49±0.05	0.00% (0/3)	0.00% (0/3)
2	0.46±0.13	33.33% (1/3)	0.00% (0/3)
3	0.57±0.03	0.00% (0/3)	0.00% (0/3)
4	0.41±0.06	0.00% (0/3)	0.00% (0/3)
5	0.54±0.08	0.00% (0/3)	0.00% (0/3)
6	0.42±0.07	0.00% (0/3)	0.00% (0/3)
Total		5.56% (1/18)	0.00% (0/18)

TABLE 7. *IN VIVO* result of grinding drill.

No.	Thickness (mm)	Pierce rate	Thick rate (>1.0mm)
1	0.63±0.19	0.00% (0/3)	0.00% (0/3)
2	0.42±0.13	0.00% (0/3)	0.00% (0/3)
3	0.45±0.15	0.00% (0/3)	0.00% (0/3)
4	0.42±0.06	0.00% (0/3)	0.00% (0/3)
5	0.49±0.05	0.00% (0/3)	0.00% (0/3)
6	0.39±0.10	0.00% (0/3)	0.00% (0/3)
Total		0.00% (0/18)	0.00% (0/18)

TABLE 8. *IN VIVO* result of ultrasonic scalpel.

No.	Thickness (mm)	Pierce rate	Thick rate (>1.0mm)
1	0.62±0.52	0.00% (0/3)	33.33% (1/3)
2	0.60±0.21	0.00% (0/3)	0.00% (0/3)
3	0.51±0.27	0.00% (0/3)	0.00% (0/3)
4	0.88±0.57	0.00% (0/3)	33.33% (1/3)
5	0.48±0.08	0.00% (0/3)	0.00% (0/3)
6	0.49±0.15	0.00% (0/3)	0.00% (0/3)
Total		0.00% (0/18)	11.11% (2/18)

different thresholds for the ELM based on the number of predicted values out of the 10 sent to it being classified as inner cortical bone (ranging from 6 to 9). When a threshold of 6 to 9 out of 10 predicted values was exceeded, stop instruction will be issued to halt the robot's movement. The final

TABLE 9. *IN VIVO* result of freehand milling.

	Pierce rate	P value of pierce rate	Thickness(mm)	P value of thickness
Grinding drill	100.00% (9/9)	2.21×10^-5**	0.00±0.00	-
Ultrasonic scalpel	77.78% (7/9)	1.75×10^-5**	1.20±0.33	0.012*

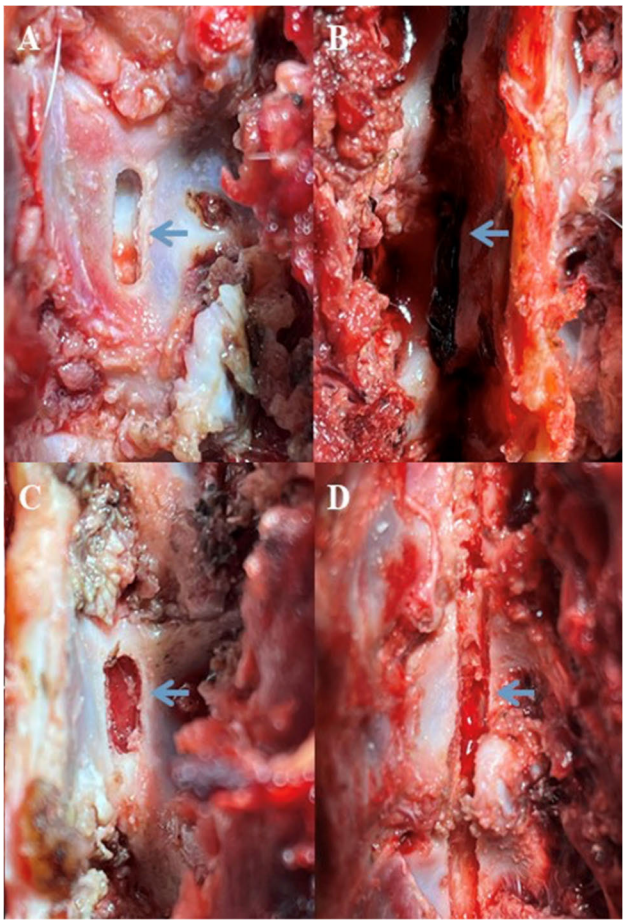

FIGURE 16. Vision observation of *IN VIVO* experiment result of robot-assist and freehand laminectomy. A. Result of robot-assist laminectomy with grinding drill; B. Result of freehand laminectomy with grinding drill; C. Result of robot- assist laminectomy with ultrasonic scalpel; D. Result of freehand laminectomy with ultrasonic scalpel. The blue arrow in the figure are the milling areas.

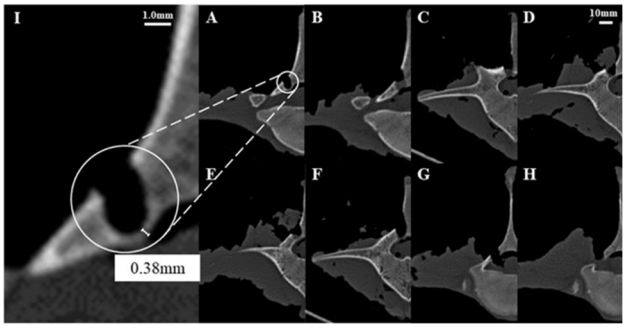

FIGURE 17. CT image of *IN VIVO* experiment result. A-D. CT image of robot-assist laminectomy (A) and freehand laminectomy of three identical doctor (B-D) with grinding drill, respectively; E-H. CT image of robot-assist laminectomy(A) and freehand laminectomy of three identical doctor (B-D) with ultrasonic scalpel, respectively.

position of the grinding instrument was confirmed through visual observation and postoperative CT scans. To determine the most suitable threshold, we examined the remaining vertebral body thickness. Different thresholds were studied for their impact on grinding efficiency and movement speed, and the average was taken for comparison. Through these in vitro experiments, we established that when the ELM identifies 8 out of the 10 predicted values as inner cortical bone, it ensures the thinnest remaining bone with relatively low penetration rates. (Fig.13) We plotted the fitting module and classification module outputs by sampling points in the in vitro experiment (Threshold: 8 of 10), and compared them with the previous experiments. The experimental results are largely consistent. Subsequently, we configured the ELM to send instructions to the robot every 10 predicted values. If 8 of these values were recognized as inner cortical bone, a stop command was issued to halt the robot's movement. Data analysis was performed for various conditions of ultrasonic bone scalpel and high-speed grinding drill (Tables 1 and 2). We observed that, in both ultrasonic scalpel group and grinding drill group, the lamina was milled to a thin layer in each condition, only two laminas was pierced (Fig 11), one of grinding drill group in 20000r/s of griding speed and 1mm/s of moving speed, the other of ultrasonic scalpel group in 80% of milling power and 0.5mm/s of moving speed. The CT image also confirmed that the grinding instrument reached the inner cortical bone and only two laminas was pierced. The residual thickness of each lamina was measured, and the average thickness of grinding drill group and ultrasonic scalpel group was 0.36±0.11mm and 0.48±0.08mm respectively (Table. 5 and Table. 6).

2) IN VIVO VERIFY EXPERIMENT

As the actual operation conditions are more complicated than in vitro experiments, we further verify the security and accuracy of our stop control strategy in vivo by live animal experiment. Four Yorkshire miniature swines, two male and

two female, were selected for this study. Each swine weighed about 40kg and was approximate 1.3m long. Fasting 24 hours before surgery, sodium pentobarbital was administered intravenously to induce anesthesia, while inhalation of isoflurane to maintain anesthesia. The vital signs of swine were monitored during the operation (Fig. 15).

After anesthesia induction, place the swine as the prone position. To maintain the stability of the spine, we fixed the swine limbs, back, buttocks with bandage. After skin preparation, disinfection and drapes spreading, surgeon incised the skin along the median dorsal incision, peeled the paravertebral muscles and other soft tissues, performed electrocautery. Expose the signature structures includes spinous process, lamina, superior and inferior articular process, of surgical area with spreaders. The milling process is the same as in vitro verify experiment, force signal will be synchronized to computer to provide a basis for real-time estimate the position of grinding instrument. Stop strategy is identical to in vitro experiment.

We also conduct freehand milling by three experienced spine surgeons. All surgeons select 100% milling power of ultrasonic scalpel and 20000r/s grinding speed of grinding drill. Each condition of robot-assist milling and freehand milling repeat operated in three laminas. According to the surgeon's custom, three designated laminas were milled continuously. After operation, euthanized the swine by air embolization, and take out the experiment segment spine. Performed visual observation and CT scan to confirmed whether the lamina was pierced, whether the residual lamina is only inner cortical bone.

In observation, most of lamina in freehand group was pierced, the slot and border of milling path was rough and variance in different surgeon. In ultrasonic scalpel group, total 9 lamina were milling by 3 surgeons, only 2 laminas milling by the same surgeon didn't pierce, while in grinding drill group, all of 9 laminas were pierced. By contrast, the milling path of robot-assist group were smooth and regular. No lamina was pierced in total 36 laminas milling by ultrasonic scalpel and by grinding drill (Fig. 16).

We further measured the residual lamina by CT image. The minimum thickness was record, and the pierced lamina were record as 0. The average and standard deviation didn't include the pierced sample (Fig. 17). The thickness of lamina milling by freehand ultrasonic scalpel is 0.80±0.33mm. In robot-assist group, the residual lamina is 0.60±0.33mm in ultrasonic scalpel and 0.47±0.13mm in grinding drill. But in two laminas of ultrasonic scalpel group, the residual thickness was more than twice that of the inner cortical bone (Table.7 and Table.8). The chi-square test was used to compare the pierce rate of robotic and freehand milling. (Table.9) The results showed that the pierce rate of freehand milling was significantly higher than that of robotic milling, and the P values of drill grinding group and ultrasonic cutter group were $2.21 \times 10{-}5$ and $1.75 \times 10{-}5$, respectively. The residual lamina thickness in ultrasonic scalpel group was thicker by freehand than by robot (P value: 0.012). Due to all of the freehand grinding drill milling penetration, so it is not comparable.

V. DISCUSSION

Laminectomy is applicable to various conditions such as disc herniation, spinal stenosis, vertebral slippage, vertebral tumor, and is one of the most common surgical approaches in spinal surgery. With the increasing application of surgical robots in surgical procedures, spinal surgery robots are also increasingly used in clinical practice. Due to the high risks associated with spinal surgery, which may result in complications such as spinal cord and nerve damage, the clinical application of spinal surgery robots is currently limited to the insertion of pedicle screws and does not involve surgical operations closely adjacent to the spinal canal. However, the key to spinal surgery lies in decompressing the spinal canal and enlarging its volume through laminectomy.

In this study, we propose a bone recognition method based on Extreme Learning Machine (ELM) and the characteristics of human bone to determine the depth of laminectomy during surgery by analyzing force signals, thereby determining whether the inner cortical bone is reached. When grinding drill or ultrasonic scalpel touch the inner cortical bone, typically within 1mm, it stop working, effectively preventing damage to the spinal cord and nerves beneath the inner cortical bone, thereby enhancing surgical safety. Meanwhile, the remaining inner cortical bone can be easily separated from the vertebral bone, achieving the purpose of laminectomy.

Based on the ELM-based method proposed in this paper, we conducted both in vitro and in vivo experiments. In vitro experiments were mainly used to determine the threshold of remaining cortical bone thickness that meets clinical satisfaction and to validate different scenarios with commonly used spinal surgical instruments such as ultrasonic scalpel and drill. We found that when the threshold was set to 8, the inner cortical bone could be effectively identified, and the remaining inner cortical bone could be easily separated from the vertebral bone under different scenarios, with high recognition rate and low risk of nerve injury.

In vivo experiments further validated the results of in vitro experiments by simulating robot-assisted laminectomy in swines and non-robot-assisted laminectomy. By comparing the two surgical processes, we confirmed the effectiveness of the proposed method in actual surgical procedures. The use of this method for robot-assisted laminectomy can preserve very little inner cortical bone without causing grinding drill or ultrasonic scalpel to enter the spinal canal, whereas non-robot-assisted laminectomy surgery often involves drills or ultrasonic scalpel entering the spinal canal, leading to potential mechanical and thermal injuries. Inexperienced surgeons are likely to damage nerves during surgery, resulting in conditions such as paralysis and sensory abnormalities.

The All-Encompassing Bone Recognition and Safety Control Strategy proposed by us is the first bone recognition and safety control strategy used in laminectomy surgery in spinal surgery. It is also the first control strategy validated

through in vitro and in vivo experiments to demonstrate that minimal inner cortical bone can be preserved during robot-assisted laminectomy surgery without completely penetrating the lamina. This control strategy is based on the use of a force sensor on the ultrasonic bone scalpel to identify the inner cortical bone, breaking through the technical challenges of this surgery, maximizing the safety of the spinal cord and nerves, refining and intelligentizing laminectomy surgery, reducing the learning curve and difficulty of the technology, and laying the foundation for future applications of robots in spinal surgery.

VI. CONCLUSION

Based on the ELM algorithm, we have developed an all-encompassing force-feedback model applicable to various milling instruments and milling conditions. This model is designed to identify the lamina's inner cortical bone, serving as the basis for our novel lamina milling safety control strategy and we have established safety control thresholds for this model. With this strategy, anchored in the model, the robot is empowered to effectuate an instantaneous cessation upon nearing the inner cortical bone, preventing penetration of the inner cortical bone and potential damage to the spinal cord and nerves beneath it. We validated the proposed theoretical results through both in vitro and in vivo animal experiments. The ELM algorithm and safety control strategy have been applied to achieve automatic control and precise control of robot-assisted lamina milling, meeting the safety control requirements in the field of medical robotics. However, this study has some limitations. For instance, we did not compensate for the periodic movement of the spine caused by respiration. Momentary respiratory micro-movements may be shorter than the feedback time of this model, potentially resulting in lamina perforation.

ACKNOWLEDGMENT

(Chengao Gao, Yu Gao, and Jiahao Li contributed equally to this work.)

REFERENCES

[1] S. Kobayashi, Y. Kokubo, K. Uchida, T. Yayama, K. Takeno, K. Negoro, H. Nakajima, H. Baba, and H. Yoshizawa, "Effect of lumbar nerve root compression on primary sensory neurons and their central branches: Changes in the nociceptive neuropeptides substance P and somatostatin," *Spine*, vol. 30, no. 3, pp. 276–282, Feb. 2005.

[2] R. W. Porter, "Spinal stenosis and neurogenic claudication," *Spine*, vol. 21, no. 17, pp. 2046–2052, Sep. 1996.

[3] G. F. Dommisse, "The blood supply of the spinal cord. A critical vascular zone in spinal surgery," *J. Bone Joint Surg. Brit.*, vol. 56, no. 2, pp. 225–235, May 1974.

[4] E. Siebert, H. Prüss, R. Klingebiel, V. Failli, K. M. Einhäupl, and J. M. Schwab, "Lumbar spinal stenosis: Syndrome, diagnostics and treatment," *Nature Rev. Neurol.*, vol. 5, no. 7, pp. 392–403, Jul. 2009.

[5] M. Hupp, N. Pfender, K. Vallotton, J. Rosner, S. Friedl, C. M. Zipser, R. Sutter, M. Klarhöfer, J. M. Spirig, M. Betz, M. Schubert, P. Freund, M. Farshad, and A. Curt, "The restless spinal cord in degenerative cervical myelopathy," *AJNR Amer. J. Neuroradiol.*, vol. 42, no. 3, pp. 597–609.

[6] G. H. Barnett, R. W. Hardy Jr., J. R. Little, J. W. Bay, and G. W. Sypert, "Thoracic spinal canal stenosis," *J. Neurosurg.*, vol. 66, no. 3, pp. 338–344.

[7] S. Duützmann, R. Fernandez, and D. Rosenthal, "Thoracic spinal stenosis: Etiology, pathogenesis, and treatment," *Der Orthopade*, vol. 48, no. 10, pp. 844–848, Oct. 2019.

[8] K. Cairns, T. Deer, D. Sayed, K. van Noort, and K. Liang, "Cost-effectiveness and safety of interspinous process decompression (superion)," *Pain Med.*, vol. 20, pp. S2–S8, Dec. 2019.

[9] D. S. Kreiner, W. O. Shaffer, J. L. Baisden, T. J. Gilbert, J. T. Summers, J. F. Toton, S. W. Hwang, R. C. Mendel, and C. A. Reitman, "An evidence-based clinical guideline for the diagnosis and treatment of degenerative lumbar spinal stenosis (update)," *Spine J., Off. J. North Amer. Spine Soc.*, vol. 13, no. 7, pp. 734–743, Jul. 2013.

[10] U. Adilay and B. Guclu, "Comparison of single-level and multilevel decompressive laminectomy for multilevel lumbar spinal stenosis," *World Neurosurg.*, vol. 111, pp. e235–e240, Mar. 2018.

[11] E. Koutsouraki, "Cerebral malformations, surgical treatment of," in *Encyclopedia of the Neurological Sciences*, 2nd ed., M. J. Aminoff and R. B. Daroff, Eds., New York, NY, USA: Academic, 2014, pp. 678–682.

[12] J. M. Rhee and S. Basra, "Posterior surgery for cervical myelopathy: Laminectomy, laminectomy with fusion, and laminoplasty," *Asian Spine J.*, vol. 2, no. 2, pp. 114–126, Dec. 2008.

[13] C. Thomé, D. Zevgaridis, O. Leheta, H. Bäzner, C. Pöckler-Schöniger, J. Wöhrle, and P. Schmiedek, "Outcome after less-invasive decompression of lumbar spinal stenosis: A randomized comparison of unilateral laminotomy, bilateral laminotomy, and laminectomy," *J. Neurosurg., Spine*, vol. 3, no. 2, pp. 129–141, Aug. 2005.

[14] Y. Chen, Z. Chang, X. Yu, R. Song, and W. Huang, "Use of ultrasonic device in cervical and thoracic laminectomy: A retrospective comparative study and technical note," *Sci. Rep.*, vol. 8, no. 1, p. 4006, Mar. 2018.

[15] Z. Li, G. Yu, S. Jiang, L. Hu, and W. Li, "Robot-assisted laminectomy in spinal surgery: A systematic review," *Ann. Transl. Med.*, vol. 9, no. 8, p. 715, Apr. 2021.

[16] Z. Deng, H. Jin, Y. Hu, Y. He, P. Zhang, W. Tian, and J. Zhang, "Fuzzy force control and state detection in vertebral lamina milling," *Mechatronics*, vol. 35, pp. 1–10, May 2016.

[17] T. Wang, S. Luan, L. Hu, Z. Liu, W. Li, and L. Jiang, "Force-based control of a compact spinal milling robot," *Int. J. Med. Robot. Comput. Assist. Surg.*, vol. 6, no. 2, pp. 178–185, Jun. 2010.

[18] Z. Deng, H. Zhang, B. Guo, H. Jin, P. Zhang, Y. Hu, and J. Zhang, "Hilbert–Huang transform based state recognition of bone milling with force sensing," in *Proc. IEEE Int. Conf. Inf. Autom. (ICIA)*, Aug. 2013, pp. 937–942.

[19] Y. Dai, Y. Xue, and J. Zhang, "Vibration-based milling condition monitoring in robot-assisted spine surgery," *IEEE/ASME Trans. Mechatronics*, vol. 20, no. 6, pp. 3028–3039, Dec. 2015.

[20] Y. Dai, Y. Xue, J. Zhang, and J. Li, "Biologically-inspired auditory perception during robotic bone milling," in *Proc. IEEE Int. Conf. Robot. Autom. (ICRA)*, May 2017, pp. 1112–1116.

[21] G.-B. Huang, Q.-Y. Zhu, and C.-K. Siew, "Extreme learning machine: A new learning scheme of feedforward neural networks," in *Proc. IEEE Int. Joint Conf. Neural Netw.*, vol. 2, Jul. 2004, pp. 985–990.

[22] A. Diker, E. Avci, E. Tanyildizi, and M. Gedikpinar, "A novel ECG signal classification method using DEA-ELM," *Med. Hypotheses*, vol. 136, Mar. 2020, Art. no. 109515.

[23] Y. Li, M. Niu, and Q. Zou, "ELM-MHC: An improved MHC identification method with extreme learning machine algorithm," *J. Proteome Res.*, vol. 18, no. 3, pp. 1392–1401, Mar. 2019.

[24] L. Wang, Z. You, D.-S. Huang, and F. Zhou, "Combining high speed ELM learning with a deep convolutional neural network feature encoding for predicting protein-RNA interactions," *IEEE/ACM Trans. Comput. Biol. Bioinf.*, vol. 17, no. 3, pp. 972–980, Oct. 2018.

[25] F. Han, C. Yang, Y.-Q. Wu, J.-S. Zhu, Q.-H. Ling, Y.-Q. Song, and D.-S. Huang, "A gene selection method for microarray data based on binary PSO encoding gene-to-class sensitivity information," *IEEE/ACM Trans. Comput. Biol. Bioinf.*, vol. 14, no. 1, pp. 85–96, Jan. 2017.

[26] P. Tan, G.-Z. Tan, Z.-X. Cai, W.-P. Sa, and Y.-Q. Zou, "Using ELM-based weighted probabilistic model in the classification of synchronous EEG BCI," *Med. Biol. Eng. Comput.*, vol. 55, no. 1, pp. 33–43, Jan. 2017.

[27] H. Qu and Y. Zhao, "Advances in tissue state recognition in spinal surgery: A review," *Frontiers Med.*, vol. 15, no. 4, pp. 575–584, Aug. 2021.

[28] F. Guan, Y. Sun, X. Qi, Y. Hu, G. Yu, and J. Zhang, "State recognition of bone drilling based on acoustic emission in pedicle screw operation," *Sensors*, vol. 18, no. 5, p. 1484, May 2018.

[29] D. J. Pell and M. Soshi, "Analysis and optimization of bone machining for robotic orthopedic surgeries," *Int. J. Med. Robot. Comput. Assist. Surg.*, vol. 14, no. 4, Aug. 2018, Art. no. e1910.
[30] H. Qu, B. Geng, B. Chen, J. Zhang, Y. Yang, L. Hu, and Y. Zhao, "Force perception and bone recognition of vertebral lamina milling by robot-assisted ultrasonic bone scalpel based on backpropagation neural network," *IEEE Access*, vol. 9, pp. 52101–52112, 2021.
[31] Y. Sun, L. Wang, Z. Jiang, B. Li, Y. Hu, and W. Tian, "State recognition of decompressive laminectomy with multiple information in robot-assisted surgery," *Artif. Intell. Med.*, vol. 102, Jan. 2020, Art. no. 101763.
[32] Z. Ying, L. Shu, and N. Sugita, "Autonomous penetration perception for bone cutting during laminectomy," in *Proc. 8th IEEE RAS/EMBS Int. Conf. Biomed. Robot. Biomechatronics (BioRob)*, Nov. 2020, pp. 1043–1048.
[33] X. Qi, Y. Sun, X. Ma, Y. Hu, J. Zhang, and W. Tian, "Multilevel fuzzy control based on force information in robot-assisted decompressive laminectomy," in *Intelligent Orthopaedics*. Singapore: Springer, 2018, pp. 263–279.
[34] G. Van Ham, K. Denis, J. V. Sloten, R. Van Audekercke, G. Van der Perre, J. De Schutter, E. Aertbeliën, S. Demey, and J. Bellemans, "Machining and accuracy studies for a tibial knee implant using a force-controlled robot," *Comput. Aided Surg., Off. J. Int. Soc. Comput. Aided Surg.*, vol. 3, no. 3, pp. 123–133, 1998.
[35] H. He, Y. Bai, E. A. Garcia, and S. Li, "ADASYN: Adaptive synthetic sampling approach for imbalanced learning," in *Proc. IEEE Int. Joint Conf. Neural Netw., IEEE World Congr. Comput. Intell.*, Jun. 2008, pp. 1322–1328.

CHENGAO GAO was born in Langfang, Hebei, in 1996. He received the B.S. degree in medicine from Zhongshan School of Medicine, Sun Yat-sen University, Guangzhou, China, in 2019. He is currently pursuing the Ph.D. degree with the Peking Union Medical College Hospital, Chinese Academy of Medical Sciences, Beijing, China. His research interests include robot-assisted spinal surgery and electronic screening and gait analysis of scoliosis

YU GAO was born in Guizhou, China, in 1996. He received the B.S. and M.E. degrees from the University of Science and Technology Beijing, Beijing, China, in 2018 and 2021, respectively, where he is currently pursuing the Ph.D. degree. His research interests include artificial intelligence, deep learning, and medical image analysis.

JIAHAO LI received the M.M. degree in surgery from Peking Union Medical College Hospital, Peking Union Medical College, Chinese Academy of Medical Sciences, Beijing, China, in 2023. He is currently working as a Postgraduate Medical Doctor with the Peking Union Medical College Hospital, Peking Union Medical College, Chinese Academy of Medical Sciences. His current research interests include orthopedic robotics, artificial intelligence, and biomedical materials.

YULONG QIN was born in Jingmen, Hubei, China, in 2000. He received the B.S. degree from the University of Science and Technology Beijing, Beijing, China, in 2022, where he is currently pursuing the M.S. degree. His research interests include artificial intelligence, autonomous driving, and 3D object detection.

YUFAN ZHAO received the B.E. degree in automation from Beijing Technology and Business University, Beijing, China, in 2019, and the M.S. degree in control engineering from the University of Science and Technology Beijing, Beijing, in 2022. She is currently working as an Assistant Engineer with the Key Laboratory of Information System and Technology, Beijing Institute of Control and Electronic Technology, Beijing. Her research interests include computer simulation and intelligent planning.

BAODUO GENG was born in Beijing, China, in 1996. He received the B.S. degree from North China Electric Power University, Beijing, in 2019, and the master's degree from Beihang University, Beijing, in 2022, where he is currently pursuing the Ph.D. degree in fundamental mathematics.

JUNCHEN WANG was born in Shenyang, Liaoning, China, in 1999. He received the bachelor's degree in clinical medicine from Capital Medical University, in 2022. He is currently pursuing the Ph.D. degree with the Peking Union Medical College Hospital, Chinese Academy of Medical Sciences. His research interests include adolescent scoliosis and spinal surgery robotics.

YONGLIANG YANG received the B.S. degree in electrical engineering from Hebei University, Baoding, China, in 2011, and the Ph.D. degree in electrical engineering from the University of Science and Technology Beijing (USTB), Beijing, China, in 2018. From 2015 to 2017, he was a Visiting Scholar at the Missouri University of Science and Technology, Rolla, MO, USA, sponsored by China Scholarship Council. He is currently working as an Associate Professor with USTB. His research interests include reinforcement learning theory, robotics, distributed optimization, and control for cyber-physical systems. He is an Associate Editor of IEEE TRANSACTIONS ON NEURAL NETWORKS AND LEARNING SYSTEMS.

DA-WEI DING (Senior Member, IEEE) received the B.E. degree from the Ocean University of China, Qingdao, China, in 2003, and the Ph.D. degree in control theory and engineering from Northeastern University, Shenyang, China, in 2010. He is currently working as a Professor with the School of Automation and Electrical Engineering, University of Science and Technology Beijing, Beijing, China. His research interests include robust control and filtering, multi-agent systems, and cyber-physical systems.

JILIANG ZHAI received the Ph.D. degree in orthopedics from the Peking Union Medical College Hospital, Chinese Academy of Medical Sciences, Beijing, China.

He is currently working as an Associate Professor and an Associate Chief Physician with the Chinese Academy of Medical Sciences, with extensive clinical experience. He has published nearly 30 papers in domestic and international journals and has been invited multiple times to give presentations at major conferences, including the Chinese Orthopedic Association Annual Meeting, and the International Society of Orthopaedic Surgery and Traumatology (SICOT). His current primary research interests include orthopedic surgical robotics and orthopedic biomaterials.

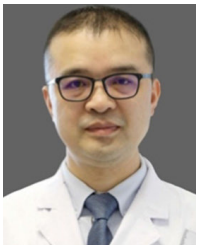

YU ZHAO was born in Shenyang, Liaoning, China, in 1970. He received the Ph.D. degree in orthopedics from the Peking Union Medical College Hospital, Chinese Academy of Medical Sciences, Beijing, China.

He is currently working as a Professor and the Chief Physician with the Department of Orthopedics, Peking Union Medical College Hospital, and works as the Ph.D. and Postdoctoral Advisor in both orthopedics and biomedical engineering. He has authored more than 190 papers in renowned international journals such as *Bioactive Materials*, *Engineering*, *Journal of Orthopaedic Translation*, and *Journal of Bone and Joint Surgery* (Am). He has also edited or co-edited 12 orthopedic books and contributed to 13 other orthopedic publications. His research interests include advanced orthopedic techniques, musculoskeletal disorders, and biomedical engineering applications in orthopedics. He is a member of the editorial boards of *Journal of Orthopaedic Translation* and Orthopaedic Surgery. He serves as the Deputy Editor for BMC Musculoskeletal Disorders.